

Dust Evolution in Population III Supernova Remnants

Takaya Nozawa*, Takashi Kozasa*, Asao Habe*, Eli Dwek[†], Hideyuki Umeda**, Nozomu Tominaga**, Keiichi Maeda[‡] and Ken'ichi Nomoto**.§

**Department of CosmoSciences, Graduate School of Science, Hokkaido University, Sapporo 060-0810, Japan*

[†]*Laboratory for Astronomy and Solar Physics, NASA Goddard Space Flight Center, Greenbelt, MD 20771*

***Department of Astronomy, School of Science, University of Tokyo, Bunkyo-ku, Tokyo 113-0033, Japan*

[‡]*Max-Planck-Institut für Astrophysik, Karl-Schwarzschild Strasse 1, 85741 Garching, Germany*

§*Research Center for the Early Universe, School of Science, University of Tokyo, Bunkyo-ku, Tokyo 113-0033, Japan*

Abstract. We present the results of calculations for the evolution of dust within Population III supernova remnants (SNRs), focusing on the dust formed in the unmixed ejecta of Type II SNe. We show that once dust grains inside the He core encounter the reverse shock, they are subject to different fates depending on their initial sizes a_{ini} . For SNRs expanding into the interstellar medium (ISM) with $n_{\text{H},0} = 1 \text{ cm}^{-3}$, grains of $a_{\text{ini}} < 0.05 \mu\text{m}$ are trapped in the hot gas and are completely destroyed; grains of $a_{\text{ini}} = 0.05\text{--}0.2 \mu\text{m}$ are trapped in the dense shell behind the forward shock with the final sizes of $0.001\text{--}0.1 \mu\text{m}$; grains of $a_{\text{ini}} > 0.2 \mu\text{m}$ are injected into the ISM without significant destruction. The total mass of surviving dust is 0.01 to $0.8 M_{\odot}$ and is higher for the lower ISM gas density. We also investigate the elemental abundances of the second-generation stars that form in the dense shell of Population III SNRs, based on the elemental composition of dust piled up in the shell. The comparison of those results with the observations of hyper-metal-poor (HMP) stars indicates that the transport of dust segregated from metal-rich gas within a SNR can be responsible for the abundance patterns of Mg and Si in HMP stars.

Keywords: dust, extinction — early universe — shock waves — supernova remnants — supernovae: general

PACS: 95.30.Lz, 95.30.Wi, 97.10.Tk, 97.20.Wt, 97.60.Bw, 98.38.Mz

INTRODUCTION

Dust grains in the early universe play crucial roles in the formation processes of stars and galaxies through the cooling of gas by their thermal emission ([1, 2]) and the formation of H_2 molecules on their surfaces ([3, 4]). In addition, the extinction of stellar light by dust causes a serious misleading in interpreting the star formation rate and the initial mass function of the very early generation of stars from the observations toward high redshifts. The extinction and thermal emission by dust grains strongly depend on their chemical compositions and size distributions. Thus, in order to elucidate the evolution of the universe from both theoretical and observational studies, it is indispensable to reveal the properties of dust in the early epoch of the universe.

Given the cosmic age less than 1 Gyr, the main sources of dust are considered to be supernovae (SNe) [5], since the dust formation in stellar winds from evolved low-mass stars requires too long timescale to supply copious amounts of dust to the interstellar medium (ISM). Some theoretical studies ([6, 7, 8, 9]) have investigated the composition, size, and mass of dust formed in the ejecta of primordial Type II SNe (SNe II) and pair-instability SNe. However, the newly condensed dust grains are subsequently processed by the reverse shock generated from the interaction of the SN ejecta with the surrounding

medium ([9, 10]). Therefore, the properties and amount of dust injected from SNe into the ISM significantly differ from those at the time of dust formation.

In this proceedings, we present the results for the evolution of the dust formed in primordial SNe by examining its processing through the collisions with the reverse shocks and its transport within SN remnants (SNRs). Our main aim is to reveal how much amount of dust can survive the reverse shock and its dependence on the progenitor mass and the ambient gas density. It is shown that a part of dust grains surviving the destruction are trapped in the dense SN shell, which may have significant impacts on the abundance patterns of the stars formed there. Thus, we investigate the elemental abundances of the second-generation stars formed in the dense shell of Population III SNRs and compare those with the observations of hyper-metal-poor (HMP) stars.

DUST EVOLUTION IN POP III SNRS

The details of calculations of the dust evolution in Population III SNRs are described in [10], where the dynamics and destruction of dust are carefully treated by taking into account the size distribution and the initial spatial distribution of each dust species. In [10], the time evolution of gas temperature and density in SNRs is calculated

for the uniform ISM with the gas temperature of 10^4 K and hydrogen number density of $n_{\text{H},0} = 0.1, 1, \text{ and } 10 \text{ cm}^{-3}$, based on the hydrodynamic models of Population III SNe by [11]. For the models of the initial dust within the He core, the results of the dust formation calculations by [7] are adopted. In this proceedings, we present the evolution of the dust formed in the unmixed ejecta of SNe II whose progenitor masses are $M_{\text{pr}} = 13, 20, 25,$ and $30 M_{\odot}$ and explosion energy is 10^{51} ergs.

Fig. 1a shows the trajectories of C, Mg_2SiO_4 , and Fe grains in the SNR for $M_{\text{pr}} = 20 M_{\odot}$ and $n_{\text{H},0} = 1 \text{ cm}^{-3}$, and Fig. 1b represents the time evolution of their sizes. In Fig. 1a, the trajectories of the forward shock, the reverse shock, and the surface of the He core are also depicted by the thick solid lines. C, Mg_2SiO_4 , and Fe grains inside the He core intrude into the reverse shock at 3650 yr, 6300 yr, and 13000 yr, respectively, and their transport and survive heavily depend on their initial sizes a_{ini} and compositions. Grains with $a_{\text{ini}} = 0.01 \mu\text{m}$ (dotted lines) are efficiently decelerated by the gas drag and are quickly trapped in the hot gas of $\geq 10^6$ K between the forward and reverse shocks. These small grains continue to be eroded by the thermal sputtering until they are completely destroyed. For grains with $a_{\text{ini}} = 0.1 \mu\text{m}$ (solid lines), the kinetic and/or thermal sputterings reduce their sizes, but the grains can survive without being completely destroyed. C and Mg_2SiO_4 grains of $a_{\text{ini}} = 0.1 \mu\text{m}$ are finally trapped in the dense SN shell formed at $\sim 2 \times 10^5$ yr with the sizes of 0.057 and $0.031 \mu\text{m}$, respectively. In the dense shell, the erosion of dust by the thermal sputtering does not work because the gas temperature drops down rapidly below 10^5 K ([12]). Fe grains of $a_{\text{ini}} = 0.1 \mu\text{m}$ are injected into the ISM because of its high bulk density, with the size of about half the initial one. Grains with $a_{\text{ini}} = 1 \mu\text{m}$ (dashed lines) can maintain their high velocities and pass through the forward shock to be injected into the ISM, undergoing the kinetic sputtering in the postshock flow; their sizes decrease only by 0.7%, 6%, and 8% of the initial ones for C, Mg_2SiO_4 , and Fe grains, respectively.

The behavior of the transport and destruction of dust within a SNR is almost independent of the progenitor mass considered here; for $n_{\text{H},0} = 1 \text{ cm}^{-3}$, grains with $a_{\text{ini}} < 0.05 \mu\text{m}$ are completely destroyed by sputtering in the hot gas, grains with $a_{\text{ini}} = 0.05\text{--}0.2 \mu\text{m}$ are piled up in the dense SN shell with the final sizes of $0.001\text{--}0.1 \mu\text{m}$, and grains with $a_{\text{ini}} \geq 0.2 \mu\text{m}$ are ejected into the ISM without being processed significantly. Accordingly, the size distribution of the surviving dust in mass is greatly populated by large sizes, compared with that at its formation. The total mass fraction of surviving dust somehow depends on the progenitor mass (Fig. 2), since the size distribution of each dust species at the time of dust formation is different from model to model.

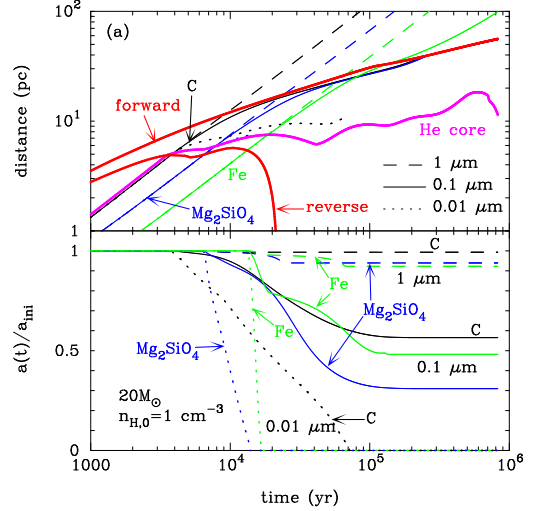


FIGURE 1. (a) Trajectories of C, Mg_2SiO_4 , and Fe grains within the SNR for $M_{\text{pr}} = 20 M_{\odot}$ and $n_{\text{H},0} = 1 \text{ cm}^{-3}$ and (b) ratios of their sizes to the initial ones as a function of time. The evolution of dust with $a_{\text{ini}} = 0.01, 0.1,$ and $1 \mu\text{m}$ is denoted by the dotted, solid, and dashed lines, respectively. The thick solid lines in (a) indicate the trajectories of the forward and reverse shocks and the position of the surface of the He core.

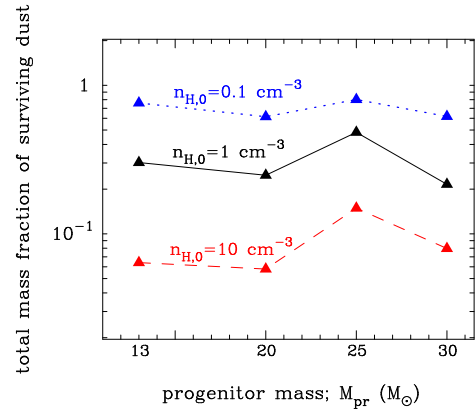


FIGURE 2. Total mass fraction of surviving dust vs. the progenitor mass. The results for $n_{\text{H},0} = 0.1, 1,$ and 10 cm^{-3} are connected by the dotted, solid, and dashed lines, respectively.

On the other hand, the ambient gas density strongly affects the evolution of dust in a SNR because the higher ISM density results in the higher density of the shocked gas and causes the efficient erosion and deceleration of dust due to more frequent collisions with the hot gas. Thus, with increasing the density in the ISM, the initial size below which dust is completely destroyed increases ($0.01, 0.05,$ and $0.2 \mu\text{m}$ for $n_{\text{H},0} = 0.1, 1,$ and 10 cm^{-3} , respectively), and the total mass fraction of the surviving dust is depressed as shown in Fig. 2. The total mass of surviving dust is $0.01\text{--}0.8 M_{\odot}$ for $n_{\text{H},0} = 10$ to 0.1 cm^{-3} .

ELEMENTAL ABUNDANCES OF THE SECOND-GENERATION STARS

Two HMP stars, HE 0107-5240 with $[\text{Fe}/\text{H}] = -5.3$ ([13, 14]) and HE 1327-2326 with $[\text{Fe}/\text{H}] = -5.45$ ([15, 16]), show extreme ($>10^2$ times) overabundances of C, N, and O and large (1–100 times) enhancements of Mg and Si relative to Fe. Recently discovered HE 0557-4880 with $[\text{Fe}/\text{H}] = -4.75$ ([17]) is also a carbon-rich ultra-metal-poor (UMP) star. Although the elemental compositions of these low-mass stars are expected to reflect the nucleosynthesis in Population III stars, the origin of the peculiar abundance patterns in HMP and UMP stars is still a matter of controversy.

The results for the evolution of dust within a SNR given in this paper show that the dust grains which survive the passage of the reverse shock but are not injected into the ISM are accumulated in the dense SN shell in 10^5 – 10^6 yr. This transport of dust to the SN shell may enable the formation of stars with solar mass scales there ([1, 2]). Thus, we investigate whether the metal abundance patterns of HMP and UMP stars can be explained by the elemental composition of dust piled up in the shell, assuming that they are the second-generation stars formed in the shell of Type II SNRs.

We present the abundances of C and O in the dense shell in Fig. 3a and those of Mg and Si in Fig. 3b, derived from the results of calculations for $M_{\text{pr}} = 20 M_{\odot}$ (filled symbols). The calculated $[\text{Fe}/\text{H}]$ is -5.20 , -5.53 , and -4.92 for $n_{\text{H},0} = 0.1$, 1, and 10 cm^{-3} , respectively, which are in good agreement with those for HMP and UMP stars. In addition, the abundances of Mg and Si for $n_{\text{H},0} = 0.1$ and 1 cm^{-3} are in the range of $0 \leq [\text{Mg}, \text{Si}/\text{Fe}] \leq 2$ and reproduce the modest overabundances of Mg and/or Si in HMP stars. Other SN models with $M_{\text{pr}} = 13$, 25, and $30 M_{\odot}$ also give the similar results for $[\text{Fe}/\text{H}]$ and $[\text{Mg}, \text{Si}/\text{Fe}]$ ([10]). Therefore, we can conclude that the transport of dust segregated from metal-rich gas within a SNR can be an important process in determining the abundance patterns of refractory elements such as Mg, Si, and Fe in the second-generation stars that form in the dense shell of primordial SNRs. It should be noted that the extreme excesses of C and O as observed in HMP stars can not be reproduced by the models considered here. Then, we examine the abundance patterns in the shell by assuming that not only the piled-up grains but also the gas outside the innermost Fe layer of the SN is incorporated into the shell. This case can produce the extreme (>100 times) overabundances of C and O but leads to unreasonable excesses of Mg and Si as well (see the open symbols in Fig. 3). However, it might be possible to reproduce the elemental abundances of HMP stars if the Si-Mg-rich layer is not mixed with the gas in the shell. This subject will be left for the future work.

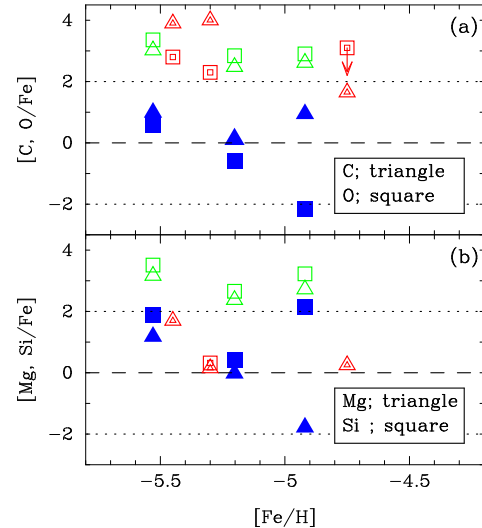


FIGURE 3. Abundances of (a) C and O and (b) Mg and Si in the shell of the SNR for $M_{\text{pr}} = 20 M_{\odot}$. The filled symbols are those from the elemental compositions of the grains piled up in the shell, and the open symbols are those including the gas outside the innermost Fe layer in addition to the piled-up grains. The observational data for HMP and UMP stars are taken from [14, 15, 16, 17, 18] and are denoted by the double symbols.

ACKNOWLEDGMENTS

This work has been supported in part by a Grant-in-Aid for Scientific Research from the Japan Society for the Promotion of Sciences (19740094 and 18104003).

REFERENCES

1. Omukai, K., et al., *ApJ*, **626**, 627–643 (2005)
2. Schneider, R., et al., *MNRAS*, **369**, 1437–1444 (2006)
3. Hirashita, H., & Ferrara, A., *MNRAS*, **337**, 921–937 (2002)
4. Cazaux, S., & Spaans, M., *ApJ*, **611**, 40–51 (2004)
5. Dwek, E., Galliano, F., & Jones, A. P., *ApJ*, **662**, 927–939 (2007)
6. Todini, P., & Ferrara, A., *MNRAS*, **325**, 726–736 (2001)
7. Nozawa, T., et al., *ApJ*, **598**, 785–803 (2003)
8. Schneider, R., Ferrara, A., & Salvaterra, R., *MNRAS*, **351**, 1379–1386 (2004)
9. Bianchi, S., & Schneider, R., *MNRAS*, **378**, 973–982 (2007)
10. Nozawa, T., et al., *ApJ in press (astro-ph/0706.0383)* (2007)
11. Umeda, H., & Nomoto, K., *ApJ*, **565**, 385–404 (2002)
12. Nozawa, T., Kozasa, T., & Habe, A., *ApJ*, **648**, 435–451 (2006)
13. Christlieb, N., et al., *Nature*, **419**, 904–906 (2002)
14. Christlieb, N., et al., *ApJ*, **603**, 708–728 (2004)
15. Frebel, A., et al., *Nature*, **434**, 871–873 (2005)
16. Aoki, W., et al., *ApJ*, **639**, 897–917 (2006)
17. Norris, J. E., et al., *submitted to ApJ (astro-ph/0707.2657)* (2007)
18. Frebel, A., et al., *ApJ*, **638**, L17–L20 (2006)